EEG - What is Possible

Stephen Chang
California State Polytechnic University, Pomona
Pomona, California, USA
stephen0.0chang@gmail.com

ABSTRACT

This paper aims to challenge the various claims in high accuracy modeling of cognitive functions such as physiological state, decision predication, and sensory modalities attributable exclusively to the statistical contribution of neural signals from non-intracranial Electroencephalograms.

We critically dissect the prevailing assumption that EEG data inherently provides meaningful insights through neural contextualization with the use of known experimental bio-electrical properties underlying neural activity and propose alternative mechanisms to account for the observed learning phenomena within these models.

ACM Reference Format:
Stephen Chang. 2025. EEG - What is Possible. In . ACM, New York, NY, USA, 8 pages. https://doi.org/10.1145/nnnnnnn.nnnnnnn

INTRODUCTION

The periodic interests in Electroencephalogram (EEG) technology, whether in consumer applications or as a futurist's promise of cognitive interpretability, necessitates an examination of theoretical and intuitive adjudicatory tools in substantiating the large academic and financial allocations towards these endeavors.

Out of numerous different techniques for neuro-imaging techniques, EEG or electroencephalograms have attracted the most attention for use in consumer devices mainly due to its high temporal resolution, relative small form factor, simple mechanics, and low cost. This, in conjunction with a rise in accessible machine learning tools, especially for processing multi-channel time series data, has led to a resurgence of academic publications for a variety of applications including as a biometric authentication, human-computer interaction layer, as well as a health device.

While models of signal propagation and cognitive theories have continuously evolved, this work seeks to exert the implications of established physical limitations and explore the conceptual foundations regarding the feasibility and coherence of interpreting neural data beyond generalized observations of neural oscillatory patterns.

1 BACKGROUND

1.1 Biological Mechanism

Neural activity, in the form of electrical impulses, is a product of bio-electrical activity. Driven by a network based on the simple biological mechanisms of neurons, astonishingly complex computational architectures form—responsible for the very basis of our unique sense of conscious experience and decision-making. The incredible study of the sources and properties of these signals highlight the exciting potential for gaining insight into the individual functionalities that underlie cognition, enabling the development of new technologies and a deeper understanding of the self.

The signals collected by the electroencephalogram (EEG) measure the aftermath of a biological process [6]. Through depolarizations events, small amounts of voltage travel through the structure from the event origination then collected by surface electrodes, amplified, and digitized for analysis.[24].

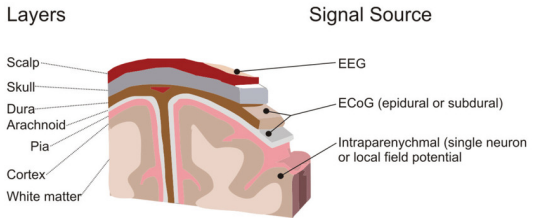

Figure 1: A Neuron [24].

The neuron is made up of several components including the cell body (soma), dendrites, axon, axon terminals, myelin sheath, nodes of Ranvier, and synapse. Each component has functions which include the capacitive storage of resting charge known as the resting potential and the release of this charge. During the resting stage, neurons release electrical charge in response to stimulation characterized by a rapid change in membrane potential (also known as depolarization). After a depolarization event, re-polarization or hyper-polarization takes place to restore the charge back to a state of resting potential[8]. The propagation of these depolarization events is transmitted through the nearby connecting cellular structures of each neuron's dendrites and axon terminals of the subsequent connected neuron. This depolarization event is the function which we measure with EEG[23].

Before we can measure electrical activity induced by depolarization events we must account for the barrier between the measured neuron and the electrode. The barriers between the skin and subsequent anatomy provide a difficult lens of observation. While intracranial techniques are favored for high-resolution observation, the invasive inconvenience of surgical procedures hinders the mass adoption of the technology.

1.2 EEG

Electroencephalograms, are devices that amplify neural electrical activity into interpretable or observable measures. First invented by

Conference'17, July 2017, Washington, DC, USA

ACM ISBN 978-x-xxxx-xxxx-x/YY/MM
https://doi.org/10.1145/nnnnnnn.nnnnnnn

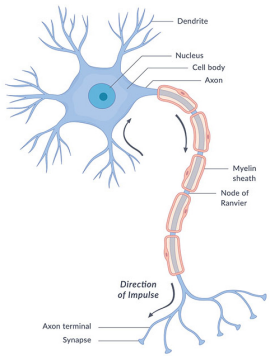

Figure 2: Structure and Layers of the Head [24].

Hans Berger in 1924, the device has been used mostly in medical applications including the detection of tumors, neuro-degenerative diseases, stroke, sleep conditions, Creutzfeldt-Jakob disease, as well as one measure of neural activity in determining cognitive death.[31]

Explorations into the observable "rhythmic" activities have resulted in surprising clarity of state information, source activity, and correlative states of mind that has solid literature that shows consistency and interpretability.[22] This paper will review the extension of these basic observations for use in much more narrow interpretations of these signal properties, specifically in addressing intent and sentiment.

1.2.1 BCI. A few interesting brain-computer interface applications to explore are in the domain of use as an input device, as an authentication method, as a measure of stimuli, and as a cognitive interface.

As an input device, EEGs have been applied in gaze estimation, intent classification, and content classification. Gaze estimation has shown promising results of around $0.1707 \pm 0.011^{\circ}$ in accuracy.[34] Intent classification has been fruitful in row-column selection in alphabet arrays and other selection-based applications by observing spikes in certain power bands. Variable dimensionality has mostly measured band power to variably controlled devices such as dials.[17] However, further refinement of these control mechanisms have faced difficulty in areas other than extremely niche control mechanisms.

As an Authentication method –there have been explorations into "thinking passwords". Unfortunately, the proposed methods to achieve this "thought to word" algorithm have not progressed further due to inherently low accuracy.[30] However, an alternative authentication method which aims to be used as an additional authentication layer by identifying users through their physiological response to audio or visual stimuli has proven much more fruitful.[9]

As a lens of decoding visual or auditory stimuli, study consistency and generalization have been few and far between due to the spatial resolution and noise of measurements.[7] It has been suggested visual stimuli may require per-neuron measurements to yield any results that can recreate or estimate the subject's direct visual experience. However, low-level classification algorithms for identifying said stimuli from a set of known class sources have yielded promising results.[35] The use of transformers in conjunction with brain signals for image generation has also been a recent development but has varying results in terms of efficacy and continuity of generated images.

1.3 Data Acquisition

The acquisition of EEG signals has evolved since its inception; however, they follow six general steps:

(1) Contact
(2) Amplification
(3) Filtering
(4) Artifact Removal
(5) Feature Extraction
(6) Training

These steps result in an end discrete digitized signal that is measured by a few qualities:

- **Spatial Resolution**: Determined by the number of electrodes and activity estimation methodology.
- **Sampling Rate**: Determined by the sampling rate of the ADC (Analog to Digital Converters).
- **Impedance**: Determined by the electrode type, hardware implementation, and chosen amplification method.
- **Noise To Signal**: Determined by the electrical soundness of the EEG setup and locality of the signal travel.

1.3.1 Electrodes. The segment of the EEG which interface between the surface of the skin and the amplification stage generally belong in the following categories:

- **Cup Electrodes**: Generally require liquid conductive paste and are taped onto the head.
- **Comb Electrodes**: Generally spiked and penetrate the hair but have high impedance due to the surface area between the spikes and the skin.
- **Polymer Electrodes**: An electrolyte-plated polymer foam which allows for dry readings with more surface area, but also has high impedance.
- **Capacitive Electrodes**: A non-contact electrode that utilizes active electrode points to amplify the electrical wave interpolation caused by neural activity.

Studies use anywhere from 8 to upwards of 250 electrodes or even high-density specialized electrodes aimed at increasing spatial resolution. The quality of raw EEG data is usually determined by three factors:

1.3.2 Amplification. The stage to allow for the signals to be observable by a ADC (analog to digital converter) can be achieved by low-noise amplifiers. There are two general methods of amplification:

- **Active**: Uses amplification on the electrode itself before a centralized amplification stage. This allows the secondary amplification stage without noise introduced in the travel from the electrode to the amplifier circuit.
- **Passive**: Uses an electrode connected to a single multi-channel centralized electronic amplification device.

Each method has its advantages and pitfalls. Between variable contact consistency, resolution, complexity, and comfort, each method

can vastly impact the form and context that the EEG can be used in.

1.3.3 Filtering. In the EEG signals collected by our aforementioned collection methods, we can observe several artifacts and sources of noise that are not of interest, such as muscle artifacts (motion, muscular, ocular, and cardiac) [3] and electrical interference (power line, device, and thermal/charge) [18].

Several methods of noise removal must be undertaken, such as simple band pass filters (high-pass filters, low-pass filters, and notch filters) for electrical interference. Furthermore, more advanced methods such as Independent Component Analysis (ICA) may be used to remove muscle artifacts.

- Bandpass Filtering – These methods will remove signal frequencies that are well-known sources of noise. Such frequencies are 50 Hz and 60 Hz, which can be mitigated by notch filters (50 Hz for non-US AC noise and 60 Hz for US AC) [18]. Furthermore, a low-pass of 100 Hz and high-pass of 0.5 Hz is used to isolate useful frequency ranges related to neural activity.
- Hardware Filtering – Before software filtering, we can ensure a cleaner dataset through RF filters, which can act to eliminate 50 Hz and 60 Hz noise. This is usually done through a twin-T filter.
- Software Filtering – Software Butterworth filter, performing a low-pass on 60 Hz, high-pass on 0.5 Hz, and a band-stop at both 50 Hz and 60 Hz.

1.3.4 Artifact Filtering. Muscle artifacts are the next challenge that we face, which are characterized by "surges in high-frequency activity" [3]. These artifacts are usually mitigated by removing by kurtosis and negentropy in components returned by Independent Component Analysis (ICA) [5].

- Independent Component Analysis – ICA is a method of linearly separating n mixed sources into n independent components. In the context of EEG signal filtering, the most common implementation FastICA, can be generalized into three distinct steps of data centering, data whitening, and data transformation. In ICA, we aim for the sources (the individual channels) of the mixed matrix to be independent and non-Gaussian.

We filter out individual components with high kurtosis and correlation, remixing the signals with the removed component for each channel.

- Empirical Mode Decomposition (EMD) – is a signal processing technique that decomposes a signal into individual Intrinsic Mode Functions (IMFs) in the time domain. An IMF is defined as a function with only one extreme between zero crossings and has a mean value of zero.

1.3.5 Features.

- Approximate Entropy – If we consider an array of data of length m and tolerance level r (which represents a fraction of the standard deviation of the EEG signals), and X_i is an array $[x_i(1), x_i(2), \ldots, x_i(m)]$ in which $x_i(k)$ represents the EEG amplitude at $i + k - 1$.
  If we compute the Euclidean distance between X_i and X_j where i and j range from 1 to $N - m + 1$, then compute the number of pairs where the distance is less than or equal to r, denoted $C_m(r)$, we then know that the approximate entropy is:

$$\mathrm{ApEn}(m, r) = \ln(C_m(r)) - \ln(C_{m+1}(r))$$

- Wavelet Entropy – We can also compute the wavelet entropy [28]. We apply a wavelet transform:

$$W(a, b) = \int_{-\infty}^{\infty} x(t)\psi_{a,b}(t)\, dt$$

  Then extract the wavelet coefficient:

$$c_{j,k} = \langle x(t), \psi_{j,k}(t) \rangle$$

  Then calculate the (Shannon) entropy with:

$$H(X) = -\sum_{i=1}^{n} p_i \log_2(p_i), \quad p_i = \frac{|c_i|^2}{\sum_{i=1}^{n} |c_i|^2}$$

- Fast Fourier Transform – a method of Fourier transform which transforms a time domain to a frequency domain. It is represented by:
  $F(\omega) = \int_{-\infty}^{\infty} f(t) e^{-i\omega t}\, dt$

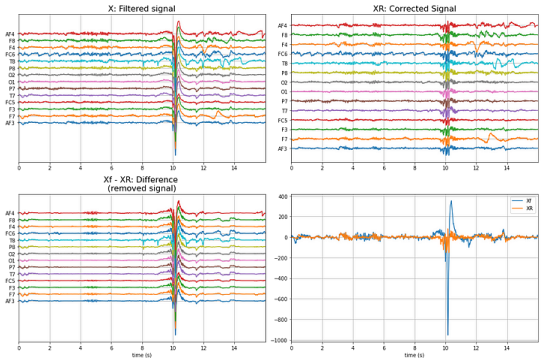

Figure 3: A Neuron [24].

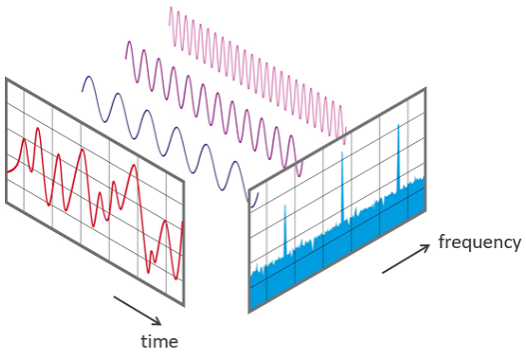

Figure 4: FFT

Where $e^{i\omega t}$ is a complex exponential function in which i is the imaginary unit and ω is the frequency parameter. The integral computes the frequency components of $f(t)$.

- Band Power – We can further dimensionally reduce the known band power by grouping the signal bands into known associated Beta, Alpha, Theta, and Delta frequency ranges, finding the power of each band for a given time frame [15]. EEG signals have classically been classified into five band classifications: Alpha (α), Theta (θ), Delta (δ), Beta (β), Gamma (γ).

Wave	Frequency Range (Hz)	State
Delta	0.5–4	Deep Sleep
Theta	4–8	Drowsiness, Dreams, Creativity
Alpha	8–15	Calmness, Relaxation, Abstract Thinking
Beta	16–31	Focus, Alertness
Gamma	32+	Perception, Short-term Memory

Table 1: Frequency Bands[22]

- Higuchi's Fractal Dimension[33] – is an estimation of the fractal dimension of a signal, measuring the complexity of a pattern. It can provide information on the dynamics and complexity of a given signal, characterizing abnormalities and non-linear dynamics.
  Given a time series, it divides the segments into varied lengths. For each segment of length k, the average length of the curve by connecting the m-th point of $[1..k]$ results in a set of curve lengths for given segments. When averaging the curve lengths, the fractal dimension is found by:

$$L_m(k) = \frac{\left\{\sum_{i=1}^{\lfloor \frac{N-m}{k} \rfloor} |x(m+ik) - x(m+(i-1)k)| \frac{N-1}{\lfloor \frac{N-m}{k} \rfloor} k\right\}}{\left\lfloor \frac{N-1}{\lfloor \frac{N-m}{k} \rfloor} k \right\rfloor} \quad (1)$$

1.3.6 Classification. Classification is a extremely wide-ranging subject area that has been extensively explored for each of the different applications and processing methods. Each has strengths and weaknesses, with a few of the most prevalent being listed below.

- Support Vector Machine (SVM) – Support Vector Machines allow for an intersection between classification and regression. It generally functions by optimizing an n-dimensional hyperplane that effectively splits the data between categories. It is effective for dimensionally large input features [10] such as EEG features. SVM has been a popular method of classification, with positive/negative classification topping around 91.77% in combination with LDA method for binary classification [26]. Furthermore, it is the most popular method, accounting for 70% of EEG classification studies [26].
  The general decision function is as follows:

$$f(x) = \text{sign}(w \cdot x + b)$$

  where:
  – w is the weight vector perpendicular to the hyperplane.

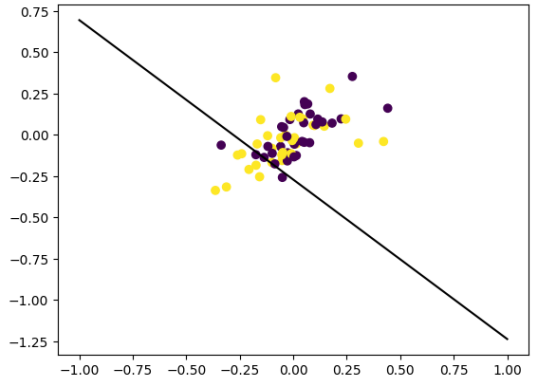

Figure 5: SVM

  – x is the input feature vector.
  – b is the bias term.
  To maximize margins between support vectors, it applies an objective function:

$$\min_{w,b} \frac{1}{2}||w||^2$$

  constrained by:

$$y_i(w \cdot x_i + b) \geq 1$$

  Soft margins can be applied by the objective function:

$$\min_{w,b} \frac{1}{2}||w||^2 + C\sum_{i=1}^{n} \xi_i$$

  constrained by:

$$y_i(w \cdot x_i + b) \geq 1 - \xi_i$$

$$\xi_i \geq 0$$

  We can also map the features into a higher dimension by using the Kernel trick:

$$f(x) = \text{sign}\left(\sum_{i=1}^{n} \alpha_i y_i K(x_i, x) + b\right)$$

  where α_i are the Lagrange multipliers of the kernel function $K(x_i, x)$.
- Recursive Neural Network (RNN) – Recursive Neural Networks function similarly to normal forward-feeding neural networks. However, there is a recursive feed of the hidden state to the previous node, allowing the network to capture temporal dynamics.
- Convolutional Neural Network (CNN) – Convolutional Neural Networks are feed-forward networks that use convolution layers to effectively extract features that are more indicative of certain characteristics. Convolution layers are field-region varied learning filters with parameter sharing between inputs that produce a two-dimensional feature map. CNNs have been an interesting approach as they can learn from local receptive fields, which allows for effective learning

from overlapping input regions. This has given hope for the use of CNNs in the highly dynamic and dimensionally complex feature set of EEG signals [36].
In a fully connected layer in a neural network:

$$y_{mn} = f(XW + b)$$

where:
- $Y_{m,n}$ is the output of the layer at (m, n).
- X represents the input matrix.
- W is the weight matrix in which w_{ij} represents the weight of the i-th input feature and j-th neuron.
- b is the bias vector b_j of the j-th neuron.

The function applied is:

$$y_{mn} = f\left(\sum_{j=0}^{J-1}\sum_{i=0}^{I-1} x_{m+i,n+j} w_{ij} + b\right)$$

where f is the activation function applied to $x_{m+i,n+j}$ input values, with w_{ij} weights of the input values, and b the bias term.

- Random Forest – Random Forest is essentially a collection of decision trees, where each tree outputs a class prediction and the class with the most votes becomes the model's prediction. It is an ensemble learning method that is effective for handling non-linear data but may struggle with high-dimensional, noisy data.

1.3.7 Review. The overwhelming quantity of different and learning algorithms provides an interesting point of comparative analysis for the effectiveness of feature-classification pairs. However, the exploration of deep neural networks may provide a path to more complex analysis of the hidden nature of neural EEG signals.

2 DISCUSSION

From the literature, we observe the litany of approaches we could take for the numerous possible applications. Our goal is to define to the best of our abilities, the limitations that EEG face in function, and challenge functional claims through mechanistic intuition or theory. We would like to present the challenge in two parts:

(1) Estimated resolution and approximate signal recovery and its implications.
(2) Statistical correlation between EMG, Facial tracking, and EEG which may better account for the observed learning.

2.1 Does Signal Recoverability Indicate Significant Capabilities?

39 million synchronously active neurons calculated as necessary to achieve a theoretical $5 - 10$ percent signal recovery would limit us to a maximum spatial resolution of approximately $2 - 5cm$ which is similar to the observed limitations of $6 - 9cm$[2].

2.1.1 Limitations in specific cognitive stimuli. Intuitively, it is then a difficult process to trace "meaningful" resolution as identifying the average signal location depends on concurrent firing of neuron clusters, but it does not allow us to trace the signal pathway. Let alone interpret the neural density to reconstruct visual stimuli given mammals such as the Etruscan shrew has neuron counts of around 1 million per hemisphere[21] which facilitates senses such as touch, smell, and vision pointing towards a factor of spatial resolution required to process visual stimuli and perhaps multiple high resolution imaging of how the brain is interpreting the visual stimuli in the estimated 4-6 billion neurons in the human visual cortex[32]. Perhaps the type of imaging required to process human visual stimuli may be exemplified by Neuralink's recent successes in using intra-cranial EEGs as a high quality input device where "System A can record 1,344 of 1,536 channels simultaneously, with the exact channel configuration arbitrarily adjustable during recording; System B can record from all 3,072 channels simultaneously"[20]. These systems achieve this using a needle density of 10.83 needles per mm^2, enabling movement resolution approximating a 100×100 grid.

While it may not be possible to interpret specific cognitive functions, the use of EEGs in sentiment analysis proposes that perhaps we can find generalized cognitive trends in certain activity types which may indicate a certain emotion or reactions. As we look into this field, we come to two important questions:

(1) How do we quantify emotions
(2) How do we interpret emotions

These questions are often reduced to a scale of valence and arousal[19] which define "valence(positive/negative, pleasant/unpleasant)[and] arousal(calm/excited)"[1] as a theory of emotional measurement. However, even with a simplified model such as this, there are not many models that can consistently provide accurate readings across different datasets and individuals. This is exemplified in a much more studied field of EEG-Text where several models have been found to have "consistent performance across EEG and random inputs rais[ing] concerns about whether the models are genuinely learning text-related information from EEG data."[13] Furthermore, there is a concern raised on how laboratory environment and the five concerns in eliciting emotion "Subject elicited vs event-elicited, lab-setting vs real-world, expression vs feeling, open-recording vs hidden-recording, and emotion-purpose vs other-purpose"[25] We can also see that generalization/individualization is a issue in these studies, resulting from a 94.38-94.72 percent accuracy rate to 68.14-63.94 percent accuracy on a binary classification[11] which would imply that while there is some amount of learning present in the model, it may be external factors such as micro-muscular movements that may be the cause of the learning, not the neural activity. Further concern on the methodology of the model training and testing is exacerbated by the often lack of a code source for replication for peer review.

2.2 Resolution

Our analysis progresses from examining the fundamental physics of neural electrical properties to interpreting the data provided by electroencephalography (EEG). Understanding the propagation of neural signals through brain tissues is crucial for developing technologies that interpret EEG signals for applications like emotion recognition.

Neurons in the cognitive areas of the brain are approximately 680×10^{-6} meters long [14]. At rest, neurons normally maintain a resting potential of -70 millivolts (mV). When a neuron is stimulated, reaching a threshold potential of -55 mV, it undergoes an

Dataset	Number of Subjects	Emotional States	Elicitation	Collected Data Types	Feature Extraction Methods	Classifiers
CK+	123	anger, contempt, disgust, fear, joy, surprise, sadness	Instruction to perform expression	Image sequences with FACS encoded	SPTS and CAPP	Linear SVM
SEED	15	positive, neutral, negative	15 emotion-specified movie clips with self-assessment	EEG, EOG, frontal face videos	STFT, differential entropy	DBN, SVM
DEAP	32	arousal, valence, liking	40 music videos with self-assessment	EEG, EMG, EOG, GSR, RSP, frontal face video	spectral power, Fisher's linear discriminant	gaussian naive bayes classifier
DECAF	30	arousal, valence	40 music videos and 36 movie clips with self-assessment	MEG, NIR facial videos, hEOG, ECG, tEMG	spectral power and DCT	Linear SVM
MPED	23	joy, funny, disgust, anger, fear, sad, neutrality	28 movie clips with self-assessment	EEG, ECG, GSR, RSP	PSD, STFT, HHS, Hjorth, HOC	SVM, KNN, LSTM, A-LSTM
PME4 (our)	11	angry, fear, disgust, sadness, happiness, surprise, natural	Instruction to perform expression	Audio, frontal face video, EMG, EEG	PCA, PSD, MFCC, autoencoder, Pre-trained CNN model	KNN, SVM, random forest, MLP, LSTM, CNN

Table 2: Overview of datasets used for emotion recognition.

action potential where the membrane potential rapidly spikes due to the influx of sodium ions.

Based on this, we can calculate the propagation model for the neural impulse signal. The electrical signal generated by neural activity must propagate through several layers before it can be collected by the EEG. The layers, along with their electrical properties, are shown in Table 3.

Tissue	Resistivity ($\Omega\,m$)	Conductivity ($S\,m^{-1}$)	Density ($kg\,m^{-3}$)
Brain	5.00	0.2381	1030
CSF	0.65	1.5380	1060
Dura (Soft Tissue)	5.76	0.1736	1050
Hard Bone	160.00	0.0063	1850
Skin	2.30	0.4348	1100

Table 3: Combined Electrical properties of various brain and tissue layers relevant to EEG signal propagation [29] Table 5 [27] Table 1.

To understand how neural activity attenuate as they propagate through different tissue layers to reach EEG electrodes, we calculate the impedance of each layer. This helps estimate the signal strength at the scalp and the number of neurons required to produce a detectable EEG signal.

2.2.1 Best Case Scenario. For low-frequency signals typical of EEG (less than 100 Hz), capacitive effects are often negligible compared to resistive effects. Using Ohm's Law, $V = I \times Z$, we calculate the minimum current I_{scalp} required at the scalp:

$$I_{\text{scalp}} = \frac{V_{\text{EEG}}}{Z_{\text{total}}} = \frac{1 \times 10^{-6}\,\text{V}}{1.01301\,\Omega} \approx 9.87 \times 10^{-7}\,\text{A} \tag{2}$$

Thus, approximately 0.987 μA of current is required at the scalp.

The signal attenuates significantly as it passes through tissue layers. Empirical studies suggest that only about 0.1% (attenuation factor $A = 0.001$) of the cortical current reaches the scalp. Considering attenuation:

$$I_{\text{cortex}} = \frac{I_{\text{scalp}}}{A} = \frac{9.87 \times 10^{-7}\,\text{A}}{0.001} = 9.87 \times 10^{-4}\,\text{A} \tag{3}$$

Therefore, approximately 987 μA of current is required at the cortical level.

Let $C_{\text{membrane}} = 1\,\mu\text{F/cm}^2$ and $A_{\text{surface}} = A_{\text{neuron}}$. Thus, each neuron contributes approximately 21 nA of current during an action potential. The number of neurons N required is calculated as:

$$N = \frac{I_{\text{cortex}}}{I_{\text{neuron}}} = \frac{9.87 \times 10^{-4}\,\text{A}}{21.36 \times 10^{-9}\,\text{A}} \approx 46,200$$

Considering a signal recovery of 1%, the adjusted number of neurons N_{adjusted} is:

$$N_{\text{adjusted}} = \frac{N}{S} = \frac{46,200}{0.01} = 4,620,000$$

Therefore, approximately 4.62×10^6 neurons need to fire synchronously.

2.2.2 Normal Case. Using the dipole moment approach, which considers the electric potential generated by neural activity in a volume conductor, we can estimate the characteristics of observable neural activity. The dipole moment p_{neuron} of a single neuron is calculated as:

$$p_{\text{neuron}} = Q \cdot d$$

where:

- $Q = 1 \times 10^{-12}$ C is the charge separation during an action potential
- $d = 680 \times 10^{-6}$ m is the length of the neuron

Calculating p_{neuron}:

$$p_{\text{neuron}} = (1 \times 10^{-12}\,\text{C}) \times (680 \times 10^{-6}\,\text{m}) = 6.8 \times 10^{-16}\,\text{C} \cdot \text{m}$$

The potential V at a distance r from a dipole p_{total} in a homogeneous volume conductor is given by:

$$V = \frac{p_{\text{total}}}{4\pi\sigma r^2}$$

Solving for p_{total} where:

- $V = 1 \times 10^{-6}$ V (detectable EEG signal)
- $\sigma = 0.33$ S/m (average conductivity of head tissues)
- $r = 0.08$ m (distance from cortical neurons to scalp)

$$p_{\text{total}} = 4\pi\sigma V r^2$$

Substituting the values:

$$p_{\text{total}} = 4\pi(0.33)(1 \times 10^{-6})(0.08)^2 = 2.65 \times 10^{-8}\,\text{C} \cdot \text{m} \quad (4)$$

Calculating the number of neurons N required:

$$N = \frac{p_{\text{total}}}{p_{\text{neuron}}} = \frac{2.65 \times 10^{-8}}{6.8 \times 10^{-16}} \approx 3.9 \times 10^7 \quad (5)$$

Approximately 39 million synchronously active neurons are needed to produce a 1 μV EEG signal at the scalp.

2.3 Is EEG Contributing to Sentiment Analysis?

When looking at EEGs, the assertion is that there are neural signals being picked up at the scalp that adds state indicative information through its measurements of neural processes. Otherwise, the cost and complex signal processing done for EEG data would not be significant towards creating a more comprehensive system for sentiment analysis.

7 category test seem to indicate little significant difference between EEG and EMG. Intuitively, EEG are just higher amplification EMG devices so if there is any learning happening from Neural Data, it should differentiate from EMG.

Type	Accuracy Range	Error Rate
EEG	15-39%	2.6%
EMG	14-37%	3.43%
Face-Tracking	15-66%	1.15%
Audio	42-69%	1.58%

Table 4: Accuracy and Error Rates for Different Modalities [4]

Type	Accuracy (%)
EEG-LSTM	86.00
Face-Tracking	89.00
Combined	93.13

Table 5: Accuracy for Different Models [12]

We can see that there seems to be little improvement co-pairing EMG and EEG data. Considering the increased signal processing and sensitivity of EEGs, it indicates the possibility that EEGs only contribute to learning due to the increased sensitivity to micromuscular activity which are oredrrs of magnitude higher in amplitude compared to actual neural activity.

Subject	KNN	SVM_Linear	SVM_Cubic	LDA
1	0.614	0.357	0.529	0.157
2	0.643	0.300	0.514	0.229
3	0.871	0.357	0.643	0.243
4	0.571	0.371	0.614	0.143
5	0.557	0.557	0.557	0.371
6	0.586	0.657	0.771	0.457
7	0.829	0.714	0.843	0.800
8	0.700	0.514	0.500	0.657
9	0.671	0.543	0.586	0.329
10	0.486	0.457	0.329	0.200
11	0.629	0.429	0.771	0.143
12	0.743	0.529	0.429	0.271
13	0.643	0.657	0.486	0.500
14	0.600	0.571	0.586	0.457
15	0.743	0.643	0.600	0.700
16	0.914	0.971	0.700	0.943
Mean	**0.675**	**0.539**	**0.591**	**0.412**

Table 6: Accuracy of Subject-Independent Classification [16]

We can further identify issues in individualization in EEG learning which is also apparent in studies utilizing EMG facial tracking based sentiment analysis; Contradicting the band based learning that seems generalized in certain features known in neural oscillations.

REFERENCES

[1] 1997. The neurobiology of emotional experience. *The Journal of Neuropsychiatry and Clinical Neurosciences* 9, 3 (1997), 439–448. https://doi.org/10.1176/jnp.9.3.439 arXiv:https://doi.org/10.1176/jnp.9.3.439 PMID: 9276845.

Subject	KNN	SVM_Linear	SVM_Cubic	LDA	Mean
1	0.971	0.829	0.900	0.829	0.882
2	0.900	0.900	0.886	0.943	0.907
3	0.986	0.971	1.000	0.857	0.954
4	0.986	0.971	0.986	0.929	0.968
5	0.929	0.886	0.943	0.914	0.918
6	0.671	0.829	0.829	0.657	0.746
7	0.929	0.929	1.000	0.929	0.946
8	0.914	0.929	0.971	0.886	0.925
9	0.957	0.943	0.957	0.929	0.946
10	0.986	0.871	0.971	0.971	0.950
11	0.986	0.986	1.000	0.957	0.982
12	1.000	0.971	0.986	0.929	0.971
13	0.943	0.886	0.971	0.900	0.925
14	0.986	0.886	1.000	0.943	0.954
15	0.957	0.986	0.986	0.957	0.971
16	0.957	0.914	0.971	0.929	0.943
Mean	**0.941**	**0.918**	**0.960**	**0.904**	**0.904**

Table 7: Accuracy of Subject-Dependent Classification [16]

[2] F Babiloni, F Cincotti, F Carducci, PM Rossini, and C Babiloni. 2001. Spatial enhancement of EEG data by surface Laplacian estimation: the use of magnetic resonance imaging-based head models. *Clinical Neurophysiology: Official Journal of the International Federation of Clinical Neurophysiology* 112, 5 (May 2001), 724–727. https://doi.org/10.1016/s1388-2457(01)00494-1

[3] C. Brunner et al. 1996. Muscle artifacts in the EEG. *Journal of Clinical Neurophysiology* 13, 2 (1996), 157–168.

[4] J. Chen, T. Ro, and Z. Zhu. 2022. Emotion Recognition With Audio, Video, EEG, and EMG: A Dataset and Baseline Approaches. *IEEE Access* 10 (2022), 13229–13242. https://doi.org/10.1109/ACCESS.2022.3146729

[5] A. Delorme and S. Makeig. 2004. EEGLAB: an open source toolbox for analysis of single-trial EEG dynamics including independent component analysis. *Journal of Neuroscience Methods* 134, 1 (2004), 9–21.

[6] G. Dornhege, J. del R. Millán, T. Hinterberger, D. McFarland, and K. R. Müller (Eds.). 2007. *Toward Brain-Computer Interfacing*. MIT Press.

[7] Matteo Ferrante, Tommaso Boccato, Stefano Bargione, and Nicola Toschi. 2024. Decoding visual brain representations from electroencephalography through knowledge distillation and latent diffusion models. *Computers in Biology and Medicine* 178 (2024), 108701. https://doi.org/10.1016/j.compbiomed.2024.108701

[8] J. Grider and K. Maloney. 2023. *Physiology, Action Potential*. StatPearls Publishing.

[9] Luis Gutierrez and Mohammad Husain. 2017. COMPOSING AN ELECTROENCEPHALOGRAPHY BIOMETRIC FOR ANDROID OS WITH EEG WORKBENCH. https://api.semanticscholar.org/CorpusID:113397953

[10] S. H. Hsu and P. H. Wang. 2022. Proliferation of machine learning in electrophysiology: applications, challenges, and future directions. *Journal of Electrocardiology* 69 (2022), 32–38.

[11] Dongmin Huang, Sentao Chen, Cheng Liu, Lin Zheng, Zhihang Tian, and Dazhi Jiang. 2021. Differences first in asymmetric brain: A bi-hemisphere discrepancy convolutional neural network for EEG emotion recognition. *Neurocomputing* 448 (2021), 140–151. https://doi.org/10.1016/j.neucom.2021.03.105

[12] H. Jiang, R. Jiao, D. Wu, and W. Wu. 2021. Emotion Analysis: Bimodal Fusion of Facial Expressions and EEG. *Computers, Materials & Continua* 68, 2 (2021), 2315–2327. https://doi.org/10.32604/cmc.2021.016832

[13] Hyejeong Jo, Yiqian Yang, Juhyeok Han, Yiqun Duan, Hui Xiong, and Won Hee Lee. 2024. Are EEG-to-Text Models Working? arXiv:2405.06459 [cs.CL] https://arxiv.org/abs/2405.06459

[14] Eric R. Kandel, James H. Schwartz, and Thomas M. Jessell. 2000. *Principles of Neural Science* (4th ed.). McGraw-Hill.

[15] L. W. Ko, R. K. Chikara, Y. K. Wang, and C. T. Lin. 2021. Spectral entropy analysis on EEG signals during perception of emotional audiovisual contents. *Frontiers in Neurorobotics* 14 (2021), 617531.

[16] M. Kołodziej, A. Majkowski, and M. Jurczak. 2024. Acquisition and Analysis of Facial Electromyographic Signals for Emotion Recognition. *Sensors* 24, 15 (2024), 4785. https://doi.org/10.3390/s24154785

[17] Dean J Krusienski and Jerry J Shih. 2011. Control of a visual keyboard using an electrocorticographic brain-computer interface. *Neurorehabilitation and Neural Repair* 25, 4 (May 2011), 323–331. https://doi.org/10.1177/1545968310382425 Epub 2010 Oct 4.

[18] S. Leske and S. S. Dalal. 2019. Reducing power line noise in EEG and MEG data via spectrum interpolation. *NeuroImage* 189 (2019), 763–776.

[19] Malek Mneimne, Alice S. Powers, Kate E. Walton, David S. Kosson, Samantha Fonda, and Jessica Simonetti. 2010. Emotional valence and arousal effects on memory and hemispheric asymmetries. *Brain and Cognition* 74, 1 (2010), 10–17. https://doi.org/10.1016/j.bandc.2010.05.011

[20] Elon Musk. 2019. An Integrated Brain-Machine Interface Platform With Thousands of Channels. *J Med Internet Res* 21, 10 (31 Oct 2019), e16194. https://doi.org/10.2196/16194

[21] RK Naumann, F Anjum, C Roth-Alpermann, and M Brecht. 2012. Cytoarchitecture, areas, and neuron numbers of the Etruscan shrew cortex. *Journal of Comparative Neurology* 520, 11 (Aug 2012), 2512–2530. https://doi.org/10.1002/cne.23053

[22] E. Niedermeyer and F. L. da Silva. 2005. *Electroencephalography: Basic Principles, Clinical Applications, and Related Fields*. Lippincott Williams & Wilkins.

[23] G. D. Norata et al. 2023. The neuron: A brief introduction to structure and function. *Neuron* 110, 1 (2023), 1–4.

[24] National Institutes of Health. 2018. *What are neurons, and what do they do?* Technical Report. NIH Publication No. 18-NS-5180.

[25] R.W. Picard, E. Vyzas, and J. Healey. 2001. Toward machine emotional intelligence: analysis of affective physiological state. *IEEE Transactions on Pattern Analysis and Machine Intelligence* 23, 10 (2001), 1175–1191. https://doi.org/10.1109/34.954607

[26] M. M. Rahman and A. Sarkar. 2021. Recognition of emotion by EEG signal analysis: a comprehensive survey. *IEEE Transactions on Affective Computing* (2021).

[27] Ceon Ramon, Jens Haueisen, and Paul Schimpf. 2006. Influence of head models on neuromagnetic fields and inverse source localizations. *Biomedical Engineering Online* 5 (February 2006), 55. https://doi.org/10.1186/1475-925X-5-55

[28] O. A. Rosso and A. Mairal. 2007. Characterization of time dynamical evolution of electroencephalographic records. *Physica A: Statistical Mechanics and its Applications* 312, 3-4 (2007), 469–504.

[29] A.I. Sabbah, Nihad Dib, and M. Al-Nimr. 2011. Evaluation of specific absorption rate and temperature elevation in a multi-layered human head model exposed to radio frequency radiation using the finite-difference time domain method. *IET Microwaves, Antennas & Propagation* 5 (July 2011), 1073–1080. https://doi.org/10.1049/iet-map.2010.0172

[30] Julie Thorpe, Paul Oorschot, and Anil Somayaji. 2005. Pass-thoughts: Authenticating With Our Minds. *IACR Cryptology ePrint Archive* 2005 (01 2005), 121. https://doi.org/10.1145/1146269.1146282

[31] Merck Manual Professional Version. [n. d.]. Electroencephalography (EEG). https://www.merckmanuals.com/professional/neurologic-disorders/neurologic-tests-and-procedures/electroencephalography-eeg. Accessed: 2024-11-16.

[32] BA Wandell, SO Dumoulin, and AA Brewer. 2007. Visual field maps in human cortex. *Neuron* 56, 2 (Oct 2007), 366–383. https://doi.org/10.1016/j.neuron.2007.10.012

[33] A. Wanliss and K. Showalter. 2022. Efficient estimation of the Higuchi fractal dimension. *Chaos, Solitons & Fractals* 152 (2022), 111355.

[34] Nina Weng, Martyna Plomecka, Manuel Kaufmann, Ard Kastrati, Roger Wattenhofer, and Nicolas Langer. 2023. An Interpretable and Attention-based Method for Gaze Estimation Using Electroencephalography. arXiv:2308.05768 [eess.SP] https://arxiv.org/abs/2308.05768

[35] Ruiqi Yang and Eric Modesitt. 2023. ViT2EEG: Leveraging Hybrid Pretrained Vision Transformers for EEG Data. arXiv:2308.00454 [cs.CV] https://arxiv.org/abs/2308.00454

[36] X. Zhao et al. 2018. A multi-branch 3D convolutional neural network for EEG-based motor imagery classification. *IEEE Transactions on Neural Systems and Rehabilitation Engineering* 26, 10 (2018), 2226–2235.